Demography of the dominant perennial grass species of a humid African savanna

Kouamé Fulgence Koffi, Aya Brigitte N'Dri, Sarah Konaré, Tharaniya Srikanthasamy, Jean-Christophe Lata, Souleymane Konaté, Marcel Konan, Sébastien Barot

Acta Oecologica xxx (xxxx) 103816

Contents lists available at ScienceDirect

Acta Oecologica

journal homepage: www.elsevier.com/locate/actoec

Demography of the dominant perennial grass species of a humid African savanna

Kouamé Fulgence Koffi [a, b, *], Aya Brigitte N'Dri [a], Sarah Konaré [b], Tharaniya Srikanthasamy [b], Jean-Christophe Lata [b, c], Souleymane Konaté [a], Marcel Konan [a], Sébastien Barot [b]

[a] UFR des Sciences de La Nature, Station d'Ecologie de Lamto/CRE, Pôle de Recherche Environnement et Développement Durable, Laboratoire d'Ecologie et du Développement Durable, Université Nangui Abrogoua, 02 BP 801 Abidjan 02, Republic of Côte d'Ivoire

[b] Sorbonne Université, UMR 7618 IEES-Paris (IRD, CNRS, Université Paris Diderot, UPEC, INRA), 4 Place Jussieu, 75005, Paris, France

[c] Department of Geoecology and Geochemistry, Institute of Natural Resources, Tomsk Polytechnic University, 30, Lenin Street, Tomsk, 634050, Russia

ARTICLE INFO

Keywords:
Demographic matrix model
Guinean savannas
Perennial tussock grass
Population growth rate
Size-classified matrix model

ABSTRACT

Perennial grasses are the main source of fuel during fires in savannas. The demography of these grasses likely varies between species although they have the same general architecture and coexist in savannas. However, very few studies compare their demography. Similarly, their demography likely varies between years because of the variability in weather condition and fire intensity. We described and compared the demography and life-cycle of the four dominant perennial grass species (*Andropogon canaliculatus, Andropogon schirensis, Hyparrhenia diplandra* and *Loudetia simplex*) of the Lamto savanna (Ivory Coast) and assessed the influence of their demographic features (stasis, fecundity, growth, fragmentation and retrogression) on this demography. Grass species were monitored over three consecutive years (2015–2016, 2016–2017 and 2017–2018) on three 5 m × 10 m plots. We used a size-classified matrix model with 5 circumference classes (3–10 cm, 10–20 cm, 20–35 cm, 35–50 cm and >50 cm). Results showed differences in the age-based parameters, asymptotic growth rates (λs) and elasticities of the λs of the grass species. The population of *A. canaliculatus, A. schirensis* and *H. diplandra* were slowly declining while *L. simplex* was significantly declining. There were noticeable year-to-year variations in the demography of these four species. The most important demographic parameter influencing λs was the stasis in all species, while retrogression and fragmentation contributed to a relative homogeneity of ages between size-classes 2 to 5. This study provides new insights about the demography of Guinean savanna grasses that could be used to describe the mechanisms of their coexistence, and inform fire management policies.

1. Introduction

In humid tropical savannas, the grass stratum is dominated by perennial C4 tussock grasses representing 75–90% of the total above ground biomass (Menaut and Abbadie, 2006; Shea et al., 1996) and is the main source of fuel for fire (Savadogo et al., 2007; Whelan, 1995). This grass community is composed of 10–15 species (Abbadie et al., 2006; Tessema et al., 2016) that have contrasting relative abundances but tend to have the same general architecture. Indeed, they consist of large tussocks (with a circumference up to 150 cm) that can exceed 2 m in height at the end of the rainy season (Koffi et al., 2019a, 2019b; Menaut and Abbadie, 2006; N'Dri et al., 2018). Though the demography of savanna trees (Hoffmann, 1999; Stokes et al., 2004) and even palm trees (Barot et al., 2000) has often been studied, the demography of these perennial grasses has been much rarely documented. Indeed, most studies using stage-classified matrix models to describe the demography of herbaceous perennials deal with forbs (Jongejans and De Kroon, 2005; Salguero-Gómez and De Kroon, 2010). Only a few studies have assessed the demography of grasses, particularly West African perennial species (Garnier and Dajoz, 2001; Schleuning and Matthies, 2009; Silva et al., 1991).

Matrix projection models are one of the most widely used tools to compare the demography and life-cycles of different animal and plant populations (Caswell, 1989; Crone et al., 2011; Silvertown et al., 1993) or of a single species in different environments (Salguero-Gómez and De Kroon, 2010; Silvertown et al., 1993). While age-classified matrix models are usually used for animals, stage or size-classified matrix models are usually used for plant populations (Caswell, 2001). These matrix

* Corresponding author. UFR des Sciences de la Nature, Station d'Ecologie de Lamto/CRE, Pôle de Recherche Environnement et Développement Durable, Laboratoire d'Ecologie et du Développement Durable, Université Nangui Abrogoua, 02 BP 801 Abidjan 02, Republic of Côte d'Ivoire.
E-mail address: fulkoffi@yahoo.fr (K.F. Koffi).

https://doi.org/10.1016/j.actao.2022.103816
Received 14 July 2021; Received in revised form 18 December 2021; Accepted 18 January 2022
1146-609/

models constitute powerful analytical tools (Barot et al., 2002; Caswell, 2001; Cochran and Ellner, 1992), especially when: (1) survival, growth and reproduction depend more on size than on age (Harvell et al., 1990), (2) there are different modes of reproduction and (3) the age of individuals is difficult to determine (Huenneke and Marks, 1987). Savanna perennial grasses are typical examples of plants exhibiting these traits (Lauenroth and Adler, 2008; O'Connor, 1993).

While we have already published data on the demographic parameters of perennial grasses of the Lamto humid savanna in center Ivory Coast (Koffi et al., 2019b), here we use this data to parameterise matrix-population models based on classes of circumference. Thus, we modeled the demography of the four dominant grass species of this savanna as there was not enough data to build equivalent models for the less abundant species. Our first goal was to understand the dynamics of the dominant grass species through the description and comparison of their demography and life-cycle. Since the four species have different mean tussock sizes (Koffi et al., 2019a) and different values for their demographic parameters (fragmentation, mortality and retrogression Koffi et al. (2019b)), we expect them to have different asymptotic growth rates and sensitivity of these growth rates to the different demographic parameters. For example, *Andropogon canaliculatus* produces larger tussocks, has higher fragmentation rates but has lower mortality rates (Koffi et al., 2019a; 2019b) than the three other species. Such demographic differences could help explain how different species, using the same resources, coexist on the long-term (Barot and Gignoux, 2004). Moreover, perennial tussock grasses are prone to retrogression (the basal circumference of a tussock decreases over the years) and a large tussock can be fragmented leading to many smaller tussocks through a kind of clonal reproduction (Koffi et al., 2019b).

Our second goal was to assess the influence of these demographic features on the demography of the grasses. Because grass age cannot be estimated using age markers such as in trees there are very few assessments of perennial grass age but see Lauenroth and Adler (2008). Estimating this age using the matrix modelling approach is therefore a good opportunity to study how long these perennial grasses live (Cochran and Ellner, 1992). Lauenroth and Adler (2008) found that the life-spans of 11 perennial grass species varied between 5 and 39 years. Our species might also present such differences in longevities.

Finally studying the demography of savanna perennial grass species is also very important because they contribute to soil fertility (Boudsocq et al., 2009; Srikanthasamy et al., 2018), the control of run-off and erosion (Durán Zuazo and Rodríguez Pleguezuelo, 2008; Kort et al., 1998), the production of good food for livestock (Harun et al., 2017) as well as a good building material (Strohbach and Walters, 2015). The sustainable management of this important source of ecosystem services requires such a demographic study, at least to determine the stability of grass communities under global change and better manage the provision of these services.

We tested the following hypotheses: (1) Grass species are all close to a demographic equilibrium because Lamto is a reserve established more than 50 years ago and because grasses are adapted to the most important disturbance, i.e. the annual fire. (2) Grass species differ by key demographic features (e.g. the mean age in each circumference class) because they have different demographic parameters. (3) Due to the inter-annual variability in rainfall and fire intensity (Soro et al., 2021; Tiemoko et al., 2020) the demography of the four species should strongly vary between years. (4) The high frequency of tussock retrogression to a smaller tussock class and reproduction by tussock fragmentation or basal tillering should blur the relation between age and circumference. Therefore, the age in the different circumference classes should be rather homogeneous.

2. Methods

2.1. Study site

This study was conducted in the Lamto Reserve, in the wettest end of the Guinean savanna domain, in Ivory Coast (6° 9' - 6° 18′ N; 5° 15' - 4° 57' W). This site is a transition zone between semi-deciduous forests and humid savannas (Lamotte and Tireford, 1988). The Lamto Reserve is characterised by a long rainy season from March to July, a short dry season in August, a short rainy season from September to November, and a long dry season from December to February. The mean annual rainfall is about 1200 mm and the mean annual temperature is about 27 °C (Tiemoko et al., 2020). During the study period (from 2015 to 2018), the mean annual rainfall was 1167 mm and the mean temperature was 29 °C. This shows that the study years were overall slightly hotter and drier than the average climate. Since the creation of the Lamto reserve in 1963, the savanna is managed by a prescribed fire that burns grass biomass each year in the middle of January.

The vegetation of Lamto is a mosaic of forests and savannas with variable shrub and tree densities. Perennial grasses dominate the herbaceous stratum (Menaut and Abbadie, 2006). About 10 species, mostly of the tribe Andropogoneae coexist in this savanna (Abbadie et al., 2006). In this study, we analysed the demography of the four dominant species: *Andropogon canaliculatus* Schumach., *Andropogon schirensis* Hochst. ex A. Rich., *Hyparrhenia diplandra* (Hack.) Stapf and *Loudetia simplex* (Nees) C.E. Hubbard (Koffi et al., 2019a).

2.2. Study plots

Three independent 5 × 10 m plots delimited in three different patches of shrubby savanna (one plot by patch, each patch being about one km away from each other) were used to monitor grass demography for four years (from 2015 to 2018) encompassing three one-year transitions: transition 1 (2015–2016), transition 2 (2016–2017) and transition 3 (2017–2018). Plots were chosen away from all recognised sources of heterogeneity such as trees, shrubs and termite mounds. These plots were submitted to the standard mid-season fire applied in mid-January.

2.3. Data collection

We conducted a systematic sampling of perennial grasses on all plots. All the tussocks of the four studied C4 grass species having more than five tillers (identification and monitoring being then possible at this stage) were permanently marked between April and May 2015 (i.e. the first year of implementation) with a metal label tied to a metal peg. The circumference of each tussock was measured at the soil surface using a measuring tape. All labelled tussocks were censused every year in May until 2018, to determine their status, i.e. dead or living. When a tussock was alive, it was determined whether it had been fragmented since the last census, i.e. whether the tussock had been divided into at least two separate tussocks. In cases of fragmentation, the number of fragments was registered, the old peg was given to the principal fragment (i.e. the fragment with the largest circumference) and the other fragments were each labelled with a new peg. The circumference (cm) at the soil surface of all living tussocks was measured. The new tussocks arising from seed germination (i.e. seedlings) were distinguished from fragments of old tussocks and old tussocks that might have been missed in preceding censuses due to their very small sizes and the absence of fire mark at their base (remains of burned stems).

To estimate grass fecundity, three tussocks of each species were randomly chosen in each size-class (see below) and each plot to count the number of seeds produced in 2016. These individuals were followed from mid-September 2016 (i.e. the beginning of seed production of the studied species) to mid-January 2016 (i.e. the fire date). This data al-

lowed assessing the linear relation between tussock circumference and the yearly seed production for each modeled grass species (Brys et al., 2005). Numbers of new tussocks were combined to seed production data to assess fecundity as the number of new tussocks produced each year by each size-class of tussocks, without assessing the germination rate, as explained in Eq. A.1. This assessment should be relatively accurate because the dispersal distance of the seeds is very low (Garnier et al., 2002) and because our plots were themselves located in the middle of relatively homogeneous grass stands, which should avoid strong biases due to boundary effects.

2.4. Demographic model

A common size-classified matrix model was parameterised for a one-year time step for each of the four C4 tussock grass species based on their circumference. We selected five size-classes as the result of the trade-off between increasing the number of size-classes to increase the precision of life-history description, and the robustness of parameter estimations that requires having enough individuals in each size-class. These classes are: 3–10 cm (the smallest tussocks measuring 3 cm in circumference), 10–20 cm, 20–35 cm, 35–50 cm and ≥50 cm. The first two classes are narrower than the others because they gather the most individuals (Koffi et al., 2019a).

The yearly tussock transitions between size-classes are shown on the life-cycle diagram (Fig. 1). These transitions are described using three matrices i.e. the survival (S), fragmentation (F) and birth (B) matrices (Eq. A.2). The survival matrix is composed of: (1) the probabilities of stasis (P_i) on the diagonal i.e. probabilities of surviving and staying in the same class i; (2) the probabilities of retrogression ($R_{i,j}$) on the upper triangle i.e. probabilities of surviving and retrogressing from a class (j) to a smaller class (i); (3) the probabilities of recruitment ($G_{i,j}$) on the lower triangle i.e. probabilities of surviving and growing from a class (j) to a larger class (i). The fragmentation matrix is a superior triangular matrix with entries ($F_{i,j}$) representing the probabilities of tussock in the size-class j to produce new tussocks in the size-class i by fragmentation. The separate tussocks resulting from the basal tillering of marked tussocks were also considered as fragments and added to fragmentation probabilities. The birth matrix, with entries (B_i) only on the first line, regroups fecundity (i.e. reproduction through seeds).

The sum of these matrices gives the transition matrix (A) that describes the contribution of each size-class to all others, with entries $a_{(i,j)}$ i.e. A = S + F + B (Eq. A.2). The number of individuals in the population at a given time is described by the vector N with entries $n_{(i)}$ representing the number of individuals in the size-class i at a time t.

Demography can thus be summarised by the equation $N_{(t+1)} = AN_{(t)}$ (Lefkovitch, 1965), where $N_{(t)}$ and $N_{(t+1)}$ are vectors of size-class abundances at time t and t + 1, respectively.

To summarise some of the results, all the entries of the transition matrix (A) were classified into four categories according to the matrix regions they occupy. (1) Stasis (P + F) i.e. the entries in the form $P_i + F_i + B_i$ and $P_i + F_i$ on the first diagonal. (2) Fecundity (R + F + B) i.e. all the matrix entries in the form $R_{i,j} + F_{i,j} + B_i$ on the first line. (3) Retrogression (R + F) i.e. the entries in the form $R_{i,j} + F_{i,j}$. (4) Growth (G) i.e. the category of the entries $G_{i,j}$ under the first diagonal.

2.5. Demographic analyses

The dominant eigenvalue of the matrix A represents the asymptotic growth rate (λ) when the stable size-class distribution has been reached (Caswell, 1989). The stable size-class distribution is reached asymptotically if the entries of the population projection matrix do not change over time.

Due to the uncertainty in the matrix parameters (because they are estimated from imperfect data), we calculated the standard error and the 95% confidence intervals of λ, using Caswell's (2001) approach assuming its normal distribution. The confidence intervals allowed testing whether the estimated λs were significantly different from 1.0.

The elasticity of λ to the matrix parameters (Caswell, 1989) were computed. Elasticity analyses give the relative contribution of the transition matrix entries to λ. It shows how much λ can change if matrix entries change (Caswell, 1989; De Kroon et al., 2000). We then charac-

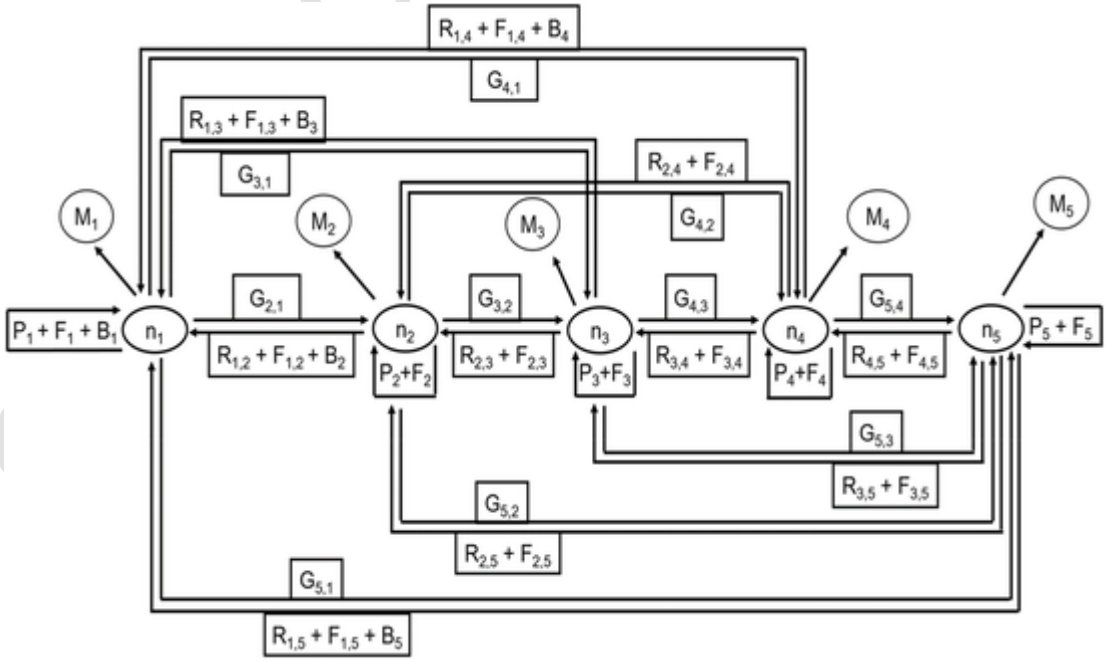

Fig. 1. Life-cycle diagram of the five size-class matrix model. The letters denote: (n) the number of individuals in each class, (M) the mortality, (G) the probability of surviving and reaching a larger size-class, (P) the probability of surviving and staying in the same size-class, (R) the probability of surviving and retrogression to a smaller size-class, (F) the probability of new tussocks apparition through fragmentation and (B) the production of new tussocks through seed production. The subscript letters (i,j) denote a transition from size-class j to size-class i (or a production of tussocks in size-class i by individuals in size-class j).

terised the life-cycle by summing the elasticities of λ over the four categories of entries (stasis, fecundity, retrogression and growth) of the transition matrix as achieved by Silvertown et al. (1992).

We conducted a log-linear analysis (Fingleton, 1984) using census data across years to test for the dependence of the transition matrices on the species, the transition years and the previous state of individuals. The response variable was the fate (i.e. the death or the new size-class of each living individual) while the explanatory variables were the species, the transition years and the state (the previous size-class of each individual). The goodness-of-fit (G^2) were calculated after adding 0.5 to each cell of the contingency tables, as suggested by Fingleton (1984).

We used life-table response experiment (LTRE) analyses to compare the demography of the species and the transition years by quantifying the contribution of each transition matrix parameter $a_{(i,j)}$ to the observed variations in λ between species and years. Contributions were calculated by the methods of Caswell (1996). The contribution of the $a_{(i,j)}$ to the difference in λ between two compared species or years was estimated by

$$\lambda^{(m)} - \lambda^{(r)} \approx \sum_{ij} \left(a_{ij}^{(m)} - a_{ij}^{(r)}\right) \left.\frac{\partial \lambda}{\partial a_{ij}}\right|_{\left(A^{(m)}+A^{(r)}\right)/2}$$

Where m and r denote the two species or years to be compared (r being the reference) and $\left.\frac{\partial \lambda}{\partial a_{ij}}\right|_{\left(A^{(m)}+A^{(r)}\right)/2}$ is the sensitivity evaluated for the mean of the two matrices i.e. at $\left(A^{(m)} + A^{(r)}\right)/2$.

The terms in the summation are the contributions of species or year differences in the matrix entries to the species or year difference in λ (Caswell, 1996). The net contribution of all $a_{(i,j)}$ to λ was calculated by summing all the entries of the contribution matrix. The comparison between species was based on the average matrix calculated over the three yearly transitions (2015–2016; 2016–2017 and 2017–2018). Although this does not predict exactly the overall growth rates of the species (Tuljapurkar et al., 2003), but it could give a general idea of the demography of each species over the three study years, which would simplify the interpretation of our results. The comparison between years was made between the yearly projection matrices of each species.

We also calculated the mean and the standard deviation of the mean age-based parameters using Cochran and Ellner method (Cochran and Ellner, 1992). This method is adequate for calculating these parameters for perennial grasses because it considers tussock fragmentation, i.e. clonal reproduction. We calculated the following age-based parameters and the corresponding standard deviations for each grass species: (1) the mean age of individuals in each size-class (y_i), (2) the mean age of residence in a class (S_i). These first two parameters differ by the fact that y_i is calculated under the assumption of the stable stage distribution but not S_i. We also calculated: (3) the mean time to first reach a class i from the class 1 ($\tau_{1,i}$), (4) the conditional remaining life-span of individuals in the class i (Ω_i) i.e. the mean remaining life-span of individuals that have reached the class i and (5) the total conditional life-span if class i has been reached (Λ_i) (Barot et al., 2002; Cochran and Ellner, 1992). The standard deviations give an idea of the variability of the age in each circumference class.

In addition, chi2 tests were performed to compare the observed size-class distribution of individuals to the predicted stable size-class distribution using the mean matrices other the three one-year transitions, with a significance level of 0.05. All these parameter calculations and analyses were achieved with the R software.

3. Results

3.1. Average matrix of the species

A total of 5853 individuals of perennial grasses were censused during the three one-year transitions. The total number of individuals by species and transition ranged from 294 for *A. schirensis* during the transition 1 to 776 for *A. canaliculatus* during the transition 3 (Table A1). Stasis were higher than all other vital rates in all species and transitions ($\chi^2 = 4619.4$; df = 24; $P < 0.001$, Table A2). Stasis varied by species and size-class ($\chi^2 = 2981.2$; df = 12; $p < 0.001$), with *A. canaliculatus* attaining its highest stasis (0.631) in class 2, whereas *A. schirensis*, *H.diplandra* and *L. simplex* attained their highest stasis, 0.673, 0.588 and 0.481, in classes 3, 4 and 1 respectively (Table A3).

The log-linear test analyzing the effects of species, transitions and the interaction on the transition matrices, based on differences in goodness-of-fit (ΔG^2) are showed in Table 1. The effects of species ($\Delta G^2 = 291.4$; df = 75; $P < 0.001$) and transitions ($\Delta G^2 = 454.4$; df = 50; $P < 0.001$) and the interaction ($\Delta G^2 = 196.7$; df = 150; $P = 0.006$) were all significant. The effects of species and transitions were significant whether or not they are combined in the calculations (Table 1). The effects of the species × transition interaction in each size-class were significant in the classes 2 and 3 ($G^2 = 56.34$; df = 30; $P = 0.002$ and $G^2 = 49.62$; df = 30; $P = 0.013$ respectively; Table 2).

3.2. Asymptotic growth rates

The mean λs, calculated with the mean transition matrices of each species were 0.9860 for *A. canaliculatus*, 0.9952 for *A. schirensis*, 0.9510 for *H. diplandra* and 0.8881 for *L. simplex*. The standard errors of the λs were 0.0321, 0.0468, 0.0374 and 0.0434, respectively. The respective 95% confidence intervals for λ under the assumption of the stable size distribution were 0.9229–1.0491, 0.9033–1.0871, 0.8776–1.0243 and 0.8030–0.9732 (Table 3). Thus, the mean λ of *L. simplex* was significantly lower than 1.0 while the λs of the other species were not significantly different from 1.0.

Table 1
Log-linear analysis of the effects of the Transition (T), Species (L) and the interaction on the demographic fate (D) of the four species, conditional on the initial state (S). G^2: goodness-of-fit; df: degree of freedom.

Model	Effects	G^2	ΔG^2	df	Δdf	p-value
DS,STL		955.3		275		<0.001
DST,STL		500.9		225		<0.001
	Transition		454.4		50	<0.001
DSL,STL		663.9		200		<0.001
	Species		291.4		75	<0.001
DST,DSL,STL		196.7		150		<0.001
	Transition		467.2		50	<0.001
	Species		304.2		75	<0.001
DSTL		0.0		0.0		1.000
	Transition × Species		196.7		150	0.006

Table 2
Log-linear analysis of the effect of the Species × Transition interaction on the fate of individuals in each size-class. G^2: goodness-of-fit values; df: degree of freedom.

State	G^2	df	p-value
Class 1	28.05	30	0.567
Class 2	56.34	30	0.002
Class 3	49.62	30	0.013
Class 4	33.19	30	0.314
Class 5	29.56	30	0.488
Total	**196.76**	**150**	**0.006**

Table 3
Population growth rates (λs) for one-year transition calculated for each grass species with associated standard errors (SE) and 95% confidence intervals. The mean values were calculated using the mean matrices of the tree one-year transitions.

	Transitions	Values of λ	SE	95% confidence interval
Andropogon canaliculatus	2015–2016	1.0545	0.0377	[0.9805, 1.1286]
	2016–2017	1.0830	0.0347	[1.0149, 1.1510]
	2017–2018	1.0722	0.0510	[0.9722, 1.1723]
	mean	**0.9860**	**0.0321**	**[0.9229, 1.0491]**
Andropogon schirensis	2015–2016	1.0443	0.0510	[0.9442, 1.1443]
	2016–2017	0.9645	0.0477	[0.8710, 1.0581]
	2017–2018	0.9426	0.0454	[0.8534, 1.0317]
	mean	**0.9952**	**0.0468**	**[0.9033, 1.0871]**
Hyparrhenia diplandra	2015–2016	1.0514	0.0454	[0.9624, 1.1405]
	2016–2017	0.9195	0.0364	[0.8482, 0.9909]
	2017–2018	0.9118	0.0350	[0.8431, 0.9804]
	mean	**0.9510**	**0.0374**	**[0.8776, 1.0243]**
Loudetia simplex	2015–2016	0.7490	0.0457	[0.6593, 0.8388]
	2016–2017	1.0722	0.0510	[0.9722, 1.1723]
	2017–2018	0.8321	0.0390	[0.7557, 0.9086]
	mean	**0.8881**	**0.0434**	**[0.8030, 0.9732]**

Contrary to the other species, the λs of *A. schirensis* were not significantly different from 1.0 during all transitions (Table 3). The λ of *A. canaliculatus* was significantly higher than 1.0 during the transition 2, but not different from 1.0 during the other transitions. The λs of *H. diplandra* and *L. simplex* were significantly lower than 1.0 respectively during the transitions 2 and 3, and during the transitions 1 and 3 (Table 3). The λs of *H. diplandra* during the transition 1 and *L. simplex* during the transition 2 were not different from 1.0 (Table 3).

3.3. Elasticity analysis

The highest elasticity in all species was for the stasis representing, on the average, 54% of the summed elasticity. These highest values of elasticity were specifically found in the classes 2, 3, 4 and 1 respectively for *A. canaliculatus* (0.295; Fig. 2A), *A. schirensis* (0.270; Fig. 2B), *H. diplandra* (0.190; Fig. 2C) and *L. simplex* (0.203; Fig. 2D). The summed elasticity of fecundity and retrogression were low (between about 3% and 17% of total elasticity; Table A4) while the summed elasticity of growth (≈23%) was intermediate. For L. *simplex*, the elasticity of fecundity and retrogression were null in the class 5. It was the same with the elasticity of the growth of small individuals of this species from the classes 1, 2 and 3 toward the class 5 (Fig. 2D).

The summed elasticity of the stasis was the highest for each species and each transition, (between 45% and 67%; Table 4). However, this highest elasticity was obtained in different classes depending on the species and transitions. The total elasticity was highest during the transition 2 for *A. canaliculatus* (63%) and *L. simplex* (57%), and the transitions 1 and 3 respectively for *A. schirensis* (67%) and *H. diplandra* (54%).

During the transition 1, the highest elasticity of the stasis was obtained in the class 3 for *A. canaliculatus* (0.319) and *A. schirensis* (0.416), in the class 4 for *H. diplandra* (0.270) and in the class 2 for *L. simplex* (0.211; Fig. A1). During the transition 2, the elasticity of stasis was highest in the classes 2, 4, 3 and 1 respectively for *A. canaliculatus* (0.405), *A. schirensis* (0.293), *H. diplandra* (0.192) and *L. simplex* (0.374; Fig. A1). This elasticity was highest for the stasis during the transition 3 in the class 2 for *A. canaliculatus* (0.265) and in the class 3 for *A. schirensis* (0.229), *H. diplandra* (0.165) and *L. simplex* (0.196) respectively. Low elasticity values were found in all species and transitions in the class 5 and for the growth of individuals towards the class 5. Therefore, the stasis was the parameter that contributed the most to the λ of all species during all transitions while fecundity had a very low contribution. Retrogression and growth contributed moderately to the λs.

3.4. Stable size distribution analysis

The highest proportions of individuals in the predicted size-class distribution were found in the classes 2 and 1 respectively for *A. canaliculatus* (44%) and *L. simplex* (43%) and the class 3 for *A. schirensis* (38%) and *H. diplandra* (31%). The lowest proportions were in the class 5 for all species (Fig. 3). The observed size distribution was significantly different from the stable size distribution in all species ($P < 0.001$ in all case). The observed proportions of individuals of *A. canaliculatus* and *L.*

Table 4
Summed values of elasticities and the corresponding proportions (%) of the total elasticity for different types of demographic parameters and transition matrices (combinations of 4 species and 3 one-year transitions, 2015–2016, 2016–2017, 2017–2018). R + F + B: Fecundity; P + F: Stasis; R + F: Retrogression; G: Growth. The species: *Andropogon canaliculatus*; *Andropogon schirensis*; *Hyparrhenia diplandra* and *Loudetia simplex*.

Species	Transitions	Summed elasticity of matrix entries				% of the summed elasticity			
		R + F + B	P + F	R + F	G	R + F + B	P + F	R + F	G
A. canaliculatus	2015–2016	0.0508	0.5713	0.1758	0.2019	5	57	18	20
	2016–2017	0.1219	0.6336	0.0558	0.1885	12	63	6	19
	2017–2018	0.0690	0.5967	0.1206	0.2135	7	60	12	21
A. schirensis	2015–2016	0.0134	0.6678	0.1557	0.1630	1	67	16	16
	2016–2017	0.0385	0.6172	0.1485	0.1956	4	62	15	20
	2017–2018	0.0344	0.5828	0.1629	0.2196	3	58	16	22
H. diplandra	2015–2016	0.0317	0.5347	0.1992	0.2342	3	53	20	23
	2016–2017	0.0821	0.5196	0.1327	0.2654	8	52	13	27
	2017–2018	0.0620	0.5355	0.1454	0.2569	6	54	15	26
L. simplex	2015–2016	0.1490	0.4536	0.1293	0.2678	15	45	13	27
	2016–2017	0.1823	0.5666	0.0379	0.2130	18	57	4	21
	2017–2018	0.1404	0.4845	0.1148	0.2601	14	48	11	26

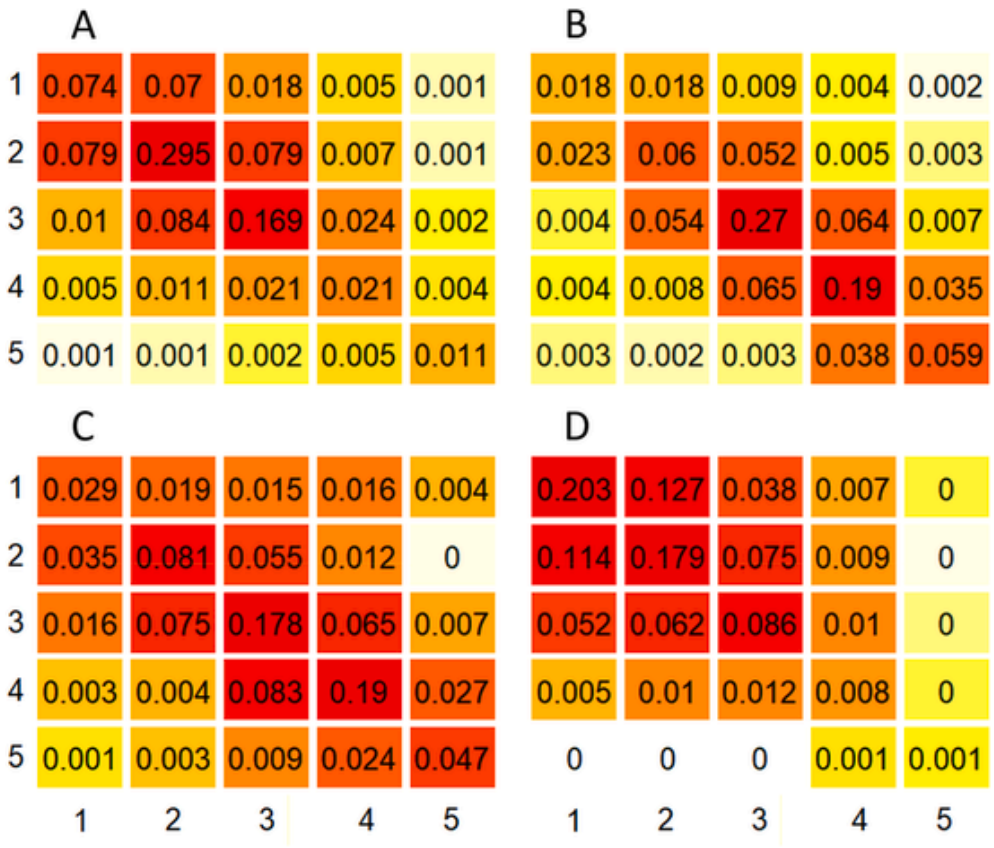

Fig. 2. Elasticity matrices of the four grass species (A: *Andropogon canaliculatus*, B: *Andropogon schirensis*, C: *Hyparrhenia diplandra* and D: *Loudetia simplex*) calculated from the mean transition matrices. The redder the colour the higher the elasticity of λ in the different size-class (1, 2, 3, 4 and 5).

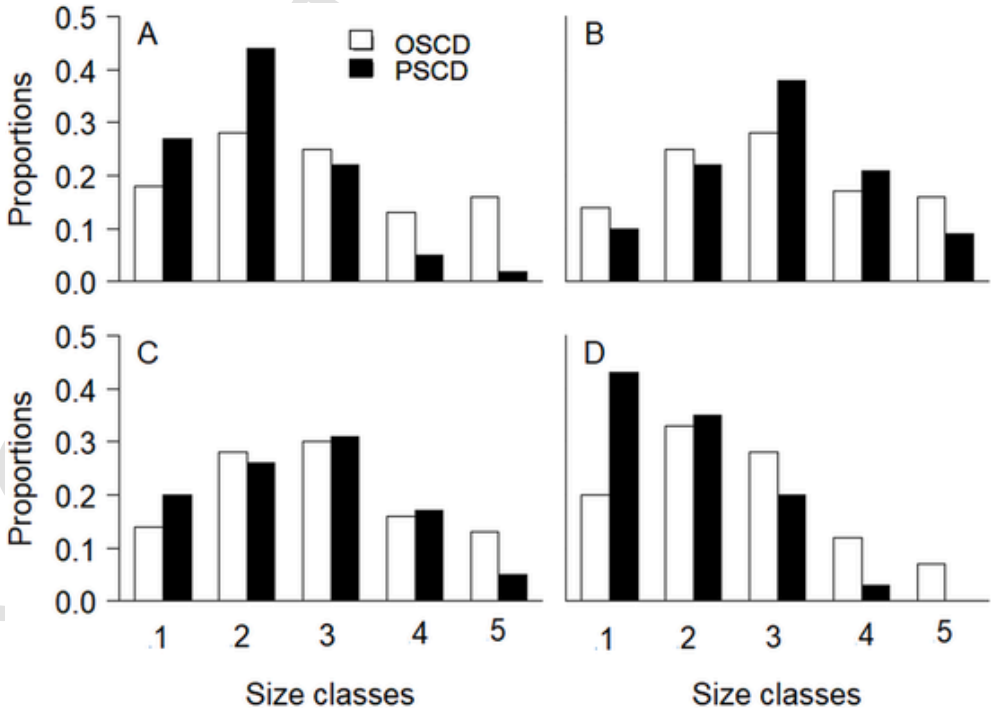

Fig. 3. Comparison of observed size-class distribution (OSCD) and predicted stable size-class distribution (PSCD) for the four species (A: *Andropogon canaliculatus*, B: *Andropogon schirensis*, C: *Hyparrhenia diplandra* and D: *Loudetia simplex*). The observed and predicted size distributions were calculated using the mean matrices of the three one-year transitions.

simplex in the classes 1 and 2 were lower than in the predicted population, while it was the reverse for the classes 3, 4 and 5 (Fig. 3A and D). This suggests that the proportion of the population in the classes 1 and 2 would increase but would decrease in the classes 3, 4 and 5, if the mean transition matrices remain constant in these species. For *H. diplandra*, the predicted proportions were higher in class 1, but lower in class 5 than the observed proportions. The two types of proportion were close in classes 2, 3 and 4. This suggests that the proportion of the population were close to the stable size distribution in the classes 2, 3 and 4, but would increase in class 1 and decrease in class 5 if the mean transition matrices remain constant in these species. The observed proportions of *A. schirensis* were higher in classes 1, 2 and 5, but lower in classes 3 and 4 than the predicted proportions meaning that there was overabundance of individuals in the classes 1, 2 and 5 and an underabundance in the classes 3 and 4.

Table 5
Life table response experiments (LTRE) comparing the four grass species (*Andropogon canaliculatus*, *Andropogon schirensis*, *Hyparrhenia diplandra* and *Loudetia simplex*). When the demographic parameters are higher in the compared species than in the reference species, contribution values are positive and vice versa. Δ λ: the difference between the asymptotic growth rates (λ) of reference species ($\lambda^{(r)}$) and compared species ($\lambda^{(c)}$); C-value: the global contribution value calculated by summing all the entries of the contribution matrix from the comparison between the corresponding species.

Reference species vs compared species	$\lambda^{(r)}$	$\lambda^{(c)}$	Δ λ	C-value
A. canaliculatus vs *A. schirensis*	0.9860	0.9952	0.0092	0.0058
A. canaliculatus vs *H. diplandra*	0.9860	0.9510	−0.0350	−0.0394
A. canaliculatus vs *L. simplex*	0.9860	0.8881	−0.0978	−0.0975
A. schirensis vs *H. diplandra*	0.9952	0.9510	−0.0442	−0.0441
A. schirensis vs *L. simplex*	0.9952	0.8881	−0.1070	−0.0967
H. diplandra vs *L. simplex*	0.9510	0.8881	−0.0628	−0.0547

3.5. LTRE analyses

3.5.1. Interspecific differences

The LTRE showed that transition matrix (and thus the demography) of the four species are significantly different (Table 5). Stasis contributed mostly (at 72%, 50% and 33%) to the differences between respectively *A. canaliculatus* and *L. simplex* (72%), *H. diplandra* and *A. schirensis* (50%) and *L. simplex* and *A. schirensis* (33%). This stasis was lower for *L. simplex* than *A. canaliculatus* and *A. schirensis* and higher for *A. schirensis* than *H. diplandra* (Fig. 4). These differences were specifically due to the stasis rates in the class 2 (*L. simplex* vs *A. canaliculatus*) and the class 3 (*L. simplex* vs *A. schirensis* and *H. diplandra* vs *A. schirensis*; Fig. A2). The differences of demography between *A. schirensis* and *A. canaliculatus* (49%), *H. diplandra* and *A. canaliculatus* (40%) and *L. simplex* and *H. diplandra* (36%) were due to differences in growth rates. *A. schirensis* and *H. diplandra* had higher growth rates than *A. canaliculatus*, whereas *L. simplex* exhibited lower growth rate than *H. diplandra* (Fig. 4). These differences were specifically due to growth in the class 2 for *A. schirensis* and *H. diplandra* and the class 3 for *L. simplex* (Fig. A2).

Taken together, the differences of demography between the four perennial grass species were mainly due to stasis and growth rates specifically in the classes 2 and 3 depending on the compared species. Fecundity (≈21% of mean contributions) and regression (≈14% of mean contributions) did not contribute much to the differences in λ between the four grass species.

3.5.2. Variations between years

The LTRE showed that there is no general pattern explaining demographic differences between yearly transitions (Fig. 5A). For *A. canaliculatus*, variations in λ were mostly influenced, at 32%, by differences in growth in the class 1 between transitions 1 and 2, at 40% to retrogression in the class 3 between transitions 1 and 3 and at 61% to stasis in

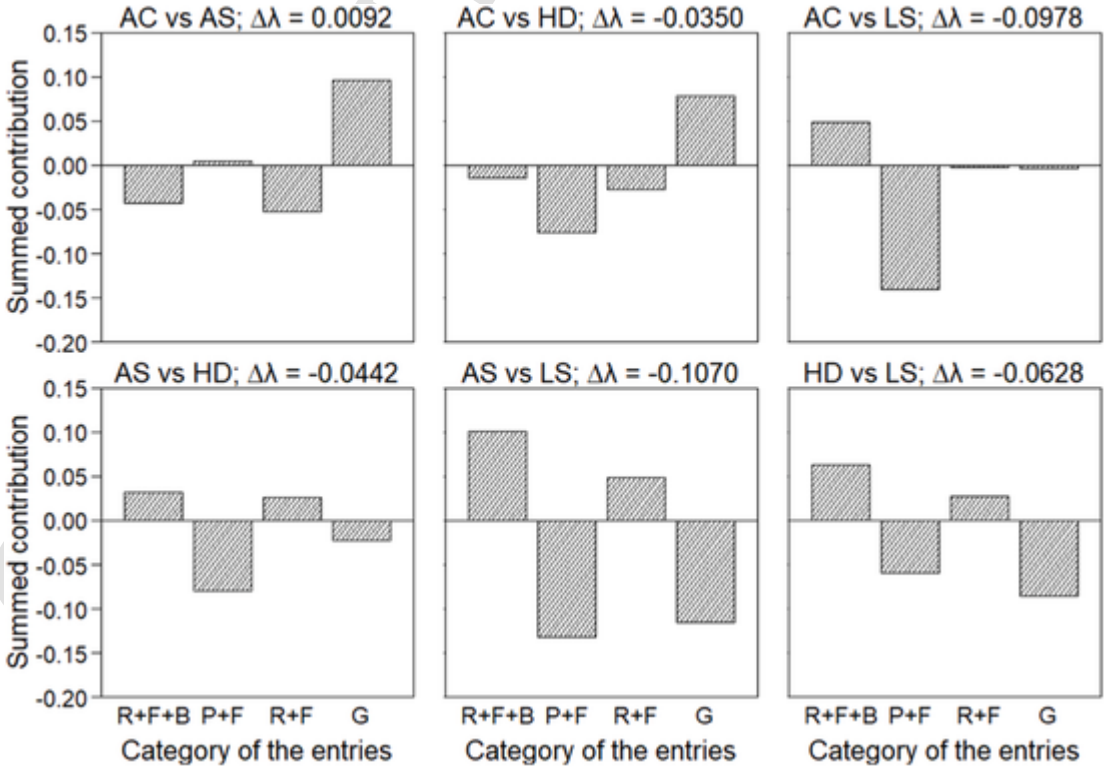

Fig. 4. The total fixed LTRE contributions of the different categories of the transition matrix entries to the species differences in λ. The categories of the demographic parameters are fecundity (R + F + B), stasis (P + F), retrogression (R + F) and growth (G). The average matrix calculated for each species over the three transitions were used. "AC vs AS" means that the parameters of the species (AS) are subtracted from those of the species (AC). Positive contribution values show that the demographic parameters are higher in the second species than in the first species and negative values show the opposite. Δλ: the difference of the growth rate (λ) between the two species. The species are AC: *Andropogon canaliculatus*; AS: *Andropogon schirensis*; HD: *Hyparrhenia diplandra*; LS: *Loudetia simplex*.

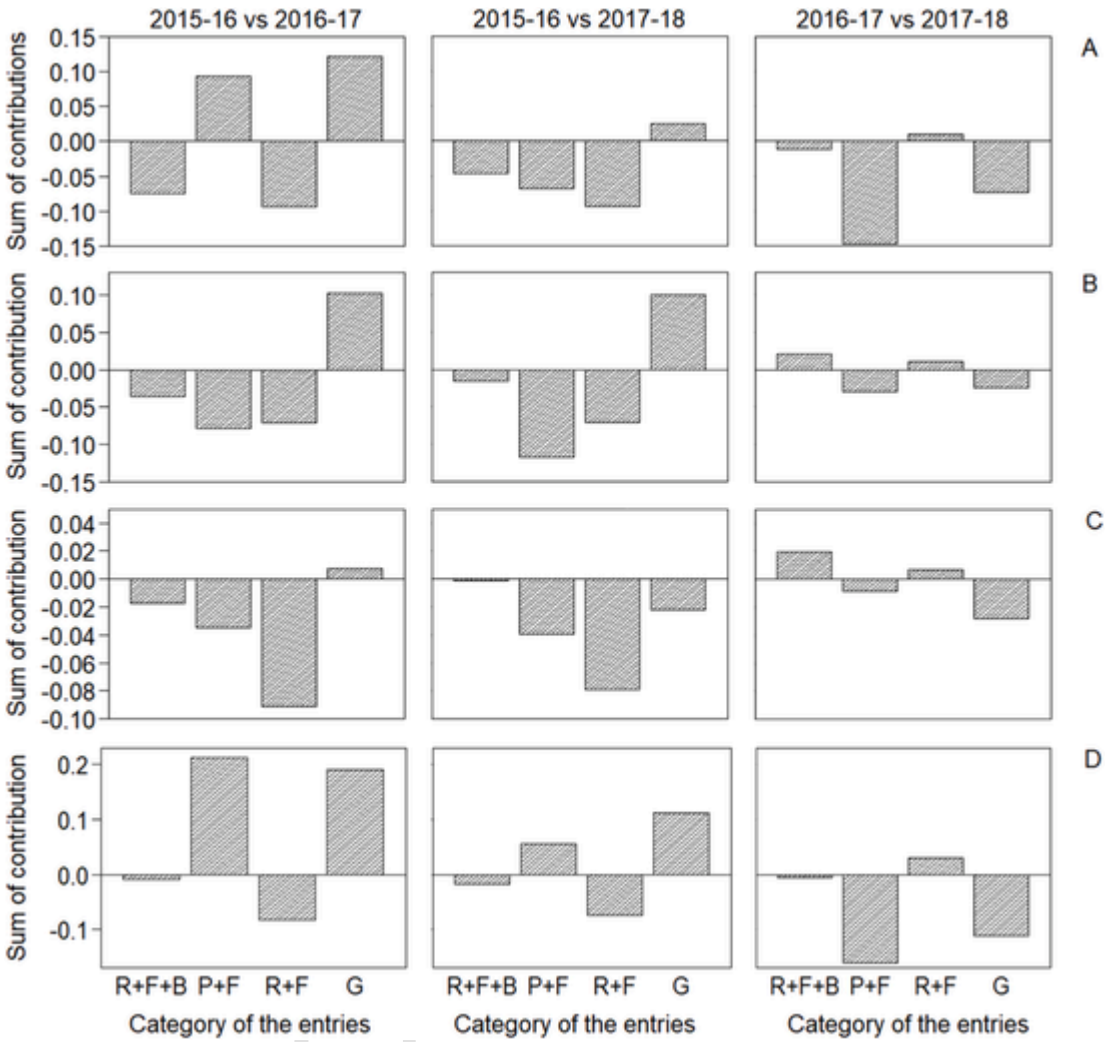

Fig. 5. The total fixed LTRE contributions of the different categories of the transition matrix entries to the differences in λ between yearly transitions for each species. The categories of the matrices are fecundity (R + F + B), stasis (P + F), retrogression (R + F) and growth (G). "2015-16 vs 2016–17" denotes that the parameters of a species in the second transition (2016–17) are subtracted from those of the first transition (2015–16). The third transition is 2017–18. Positive contribution values show that the demographic parameters are higher in the second transition than in the first transition, and negative values show the opposite. The species are in the rows A: *Andropogon canaliculatus*, B: *Andropogon schirensis*, C: *Hyparrhenia diplandra* and D: *Loudetia simplex*.

the class 2 between transitions 2 and 3 (Table A5 and Fig. A3). There was a higher growth rate during the transition 2 than transition 1, a higher retrogression rate during transition 1 than 3 and a higher stasis rate during transition 2 than 3 (Fig. 5A).

For *A. schirensis,* variations in λ were mostly influenced, at 38%, by differences in the stasis between the transitions 1 and 3 in the class 3 and, at 34%, between the transitions 2 and 3 in the class 4. The difference of λ between the transitions 1 and 2 was mostly due to differences in growth, at 36%, especially in the class 4 (Table A5 and Fig. A3). The stasis rate was lower during the transition 3 than the transitions 1 and 2 while the growth rate was higher during the transition 2 than 1 (Fig. 5B).

For *H. diplandra*, differences in λ were mostly influenced by a higher retrogression during the transition 1 than the transitions 2 and 3 (respectively at 61% and 56%). The difference of λ between the transitions 2 and 3 was mostly due to differences in growth (at 44%), especially in the class 1 (Table A5 and Fig. A3). This growth rate was higher during the transition 2 than 3 (Fig. 5C).

For L. *simplex* (Fig. 5D), the differences of λ between the transitions 1 and 2 and between the transitions 2 and 3 were due to differences in stasis (at respectively 43% and 52%) particularly in the class 1 (Table A5 and Fig. A3). This stasis was higher during the transition 2 than the transitions 1 and 3. The growth especially in the class 2 was the parameter that mostly (at 43%) influenced the difference of λ between the transitions 1 and 3 (Fig. A3). This growth rate was higher during the transition 3 than 1 (Fig. 5D). Taken together, interannual differences in fertility contributed very little to interannual differences in λ, whatever the transition or species.

3.6. Age-based parameters

The mean age of individuals in different size-classes differed by species. In each size-class, *A. schirensis* was older than other species with age ranging from 41 to 75 years and at least twice higher than for *H. diplandra* and *L. simplex* (Table 6). These two species had nearly the same mean age in the class 5 (34 years). The second oldest species in each size-classes was *A. canaliculatus* (31–43 years). In all species, the mean age of the individuals and the mean ages of residence in the classes tended to increase from class 1 to class 5 but the increase was very small from class 2 to 5. *A. schirensis* resided longer in each class than the other species while *A. canaliculatus* reached more quickly the classes 3, 4 and 5 from the class 1 (Table 6). This shows that *A. canaliculatus* grew less quickly than *A. schirensis* from the class 3 to 5. Moreover, the mean time to first reach the ith class from the class 1 ($\tau_{1,i}$) was lower

Table 6
Age-based life-history parameters of the average matrix model for the four grass species. Values are mean ± standard deviation. y_i = mean age in each size-class under the hypothesis of stable size distribution, S_i = mean age of residence in the ith class, $\tau_{1,i}$ = mean time to first reach the ith class from the class 1, Ω_i = the conditional remaining life-span of individuals in the ith class and Λ_i = total conditional life-span if class i have been reached. Calculations are based on the average matrix calculated over the three monitored one-year transitions.

	y_i	S_i	$\tau_{1,i}$	Ω_i	Λ_i	$\Omega_i/\tau_{1,i}$
Andropogon canaliculatus						
Class 1	31.2 ± 37.5	18.7 ± 23.7	7.0 ± 11.3	15.2 ± 38.4	22.2 ± 49.7	2.8
Class 2	39.5 ± 38.4	26.0 ± 24.9	4.7 ± 3.9	26.7 ± 49.0	31.4 ± 53.0	5.6
Class 3	41.7 ± 38.5	28.1 ± 25.0	9.3 ± 7.1	31.4 ± 52.5	40.8 ± 59.5	3.4
Class 4	41.5 ± 38.5	27.9 ± 25.0	20.6 ± 18.3	29.3 ± 51.3	49.9 ± 69.7	1.4
Class 5	42.8 ± 38.6	29.2 ± 25.1	25.1 ± 22.4	27.1 ± 49.9	52.2 ± 72.3	1.1
Andropogon schirensis						
Class 1	41.3 ± 63.7	27.4 ± 45.5	15.9 ± 31.9	24.4 ± 61.8	40.3 ± 93.6	1.5
Class 2	66.4 ± 70.6	48.8 ± 52.5	14.1 ± 17.7	35.0 ± 72.2	49.0 ± 89.9	2.5
Class 3	73.4 ± 70.9	55.5 ± 53.0	7.6 ± 6.1	55.2 ± 85.8	62.8 ± 91.9	7.3
Class 4	74.8 ± 71.1	56.8 ± 53.0	11.1 ± 8.7	72.3 ± 93.0	83.4 ± 101.7	6.5
Class 5	74.6 ± 71.1	56.6 ± 53.1	23.4 ± 21.4	59.0 ± 88.5	82.5 ± 109.9	2.5
Hyparrhenia diplandra						
Class 1	14.3 ± 24.3	4.3 ± 7.7	2.7 ± 5.8	5.8 ± 25.0	8.6 ± 30.8	2.1
Class 2	27.6 ± 29.1	10.9 ± 11.2	6.1 ± 6.5	8.8 ± 32.2	14.8 ± 38.7	1.4
Class 3	31.2 ± 29.5	13.6 ± 11.8	5.9 ± 4.4	12.8 ± 40.1	18.7 ± 44.6	2.2
Class 4	33.9 ± 29.7	15.9 ± 12.1	8.2 ± 5.3	18.3 ± 49.0	26.5 ± 54.3	2.2
Class 5	34.2 ± 29.7	16.1 ± 12.1	12.4 ± 9.5	15.6 ± 46.4	28.1 ± 55.8	1.2
Loudetia simplex						
Class 1	28.1 ± 29.7	5.6 ± 6.2	2.2 ± 2.7	6.5 ± 38.7	8.7 ± 41.4	2.9
Class 2	31.7 ± 29.9	8.3 ± 6.6	4.8 ± 3.3	7.7 ± 42.7	12.5 ± 46.4	1.6
Class 3	31.9 ± 29.9	8.5 ± 6.6	6.3 ± 4.7	7.1 ± 41.0	13.4 ± 45.7	1.1
Class 4	32.5 ± 29.9	9.0 ± 6.6	8.5 ± 6.4	7.4 ± 42.2	16.0 ± 45.6	0.9
Class 5	34.1 ± 29.9	10.6 ± 6.7	10.0 ± 6.6	7.9 ± 43.8	17.9 ± 50.5	0.8

in *H. diplandra* and *L. simplex* than in *A. schirensis* and *A. canaliculatus*. Thus *H. diplandra* and *L. simplex* grew quicker from class to class than *A. schirensis* and *A. canaliculatus*. Using the conditional total life-span of individuals that had reached the class 5 (Λ_5), the life-span of grasses followed this order *A. schirensis* (82.5 y), *A. canaliculatus* (52.2 y), *H. diplandra* (28.1 y), *L. simplex* (17.9 y).

All the standard deviations of the mean age in each size-class (y_i) and the mean age of residence in the ith class (S_i) increased from class 1 to class 5, for all species, due to the accumulation of uncertainties on the time of recruitment between classes. There was no precise order in the variations of the standard deviation between classes for the mean time to first reach the ith class from the class 1 ($\tau_{1,i}$), the conditional remaining life-span of individuals in the ith class (Ω_i) and the total conditional life-span if class i has been reached (Λ_i). Together with the slow increase in the mean age of individuals and the mean age of residence between class 2 and 5, this is probably due to the high retrogression rates.

4. Discussion

4.1. Are the grass species close to their demographic equilibrium?

The mean λs were lower than 1.0 for all species but only significantly for *L. simplex*. This suggests unlike Garnier and Dajoz (2001) that the population of *L. simplex* we studied was declining very quickly (by ≈ 12% a year) and would tend towards extinction. The absence of significant decline for the populations of the 3 other species can be explained by their adaptation to fire, which is a constitutive factor of all West African humid savannas (Murphy and Bowman, 2012; Sankaran et al., 2005). Up to our knowledge there has not been any other major disturbance in Lamto savanna that could locally threaten grass species. The fact that *L. simplex*, which is also a fire-adapted species, was declining (at least temporarily during the study year) could be due to its lower drought tolerance (Brink and Achigan-Dako, 2012). Indeed, the study period was slightly hotter and drier (29 °C and 1169 mm of rain) compared to the usual climate of the Lamto reserve (27 °C and 1200 mm of rain). This could increase the fragmentation and size-dependent mortality as in Butler and Briske (1988). The decline of *L. simplex* could also be due to an unfavorable plant-plant competition with the other species (Ariza and Tielbörger, 2011) because the tussocks of this species are overall smaller than the other species (Koffi et al., 2019a) and are thus shaded by the larger species, which can increase their mortality. In any case, because we are not aware of any long-term decline of *L. simplex* at the scale of Lamto savanna, the decline we have observed is probably local and temporary. This is linked to a general shortcoming of our approach (and of matrix models). Demographic parameters vary between year and between sub-populations and our predictions only describe the asymptotic demographic behavior and thus depend on such a variability. The prediction would thus require more years of census and more monitored individuals to be more robust.

4.2. Demographic differences between the grass species

As in Moloney (1988) about *Danthonia sericea*, a perennial grass species in North Carolina, and as shown by elasticities, stasis was the type of demographic parameter that most influenced our grass population growth rates. The differences of demography between the species were materialised by the fact that stasis was the highest in different size-class for each species. This suggests that the most limiting demographic parameter for each species corresponded to different size-classes. In our model, stasis gathers individuals that survive in a class and those that enter this class by fragmentation, retrogression, recruitment and germination of a seed, all these parameters depending on tussock size (Koffi et al., 2019b) and thus the size-class of the matrices. This also means that all these demographic processes jointly determined the between species differences in the most influential size-class.

Koffi et al. (2019a) classified the grass species in three groups according to their tussock size: large species (*A. canaliculatus* and *H.*

diplandra), medium size species (*A. schirensis*) and small species (*L. simplex*). For the small size species such as *L. simplex*, survival, recruitment and reproduction by seeds tend to be lower but this is compensated by low retrogression and fragmentation rates. This is due to the fact that survival, retrogression and fragmentation overall increase with the size of individuals (Koffi et al., 2019b). This could explain why *L. simplex* had highest proportional sensitivity to its highest stasis in class 1. In species with large tussocks such as *A. canaliculatus* and *H. diplandra*, probabilities of moving between classes are high. Thus, these species are likely to have strong stasis in each intermediate class (2, 3 and 4) as we can see in our matrices. However, the fact that the highest stasis occurs in different size-classes for different species could be explained for *A. canaliculatus* by a higher retrogression and fragmentation than growth from class 3 to 5. This would tend to reduce the size of the majority of individuals to class 2 and to increase the proportional sensitivity of the population demography to these small individuals. Unlike *A. canaliculatus*, *H. diplandra* exhibits higher growth than retrogression and fragmentation therefore, individuals would tend to be larger, leading to high elasticity to the highest rate of stasis in class 4. The same type of process would tend to reduce the size of individuals of *A. schirensis* towards class 3. Individuals smaller than 20 cm in circumference would grow quickly while those with more than 35 cm in circumference would undergo more fragmentation and retrogression. This would explain why this species has highest elasticity to the stasis in class 3.

The grass species also differed in all the age-based parameters. Indeed, some species grow quicker, spend more time in particular size-classes or live longer than others. Overall, the variations in the demography of the four coexisting species remain difficult to explain. According to the literature, it may depend on their taxonomic grouping and their life-form (Buckley et al., 2010; Burns et al., 2010). In our case, all species have the same life-form and are from the Andropogoneae taxonomic tribe so that the demographic differences are difficult to explain. Our results suggest that our four species highly differ in their total conditional life-span, which seems to be in relation with the λs of the species. Indeed, *A. schirensis* (82.5 y with $\lambda = 0.9952$) lives longer than *A. canaliculatus* (52.2 y with $\lambda = 0.9860$) that lives longer than *H. diplandra* (28.1 y with $\lambda = 0.9510$) that lives longer than *L. simplex* (17.9 y with $\lambda = 0.8881$). This is consistent with García et al., (2008) who observed that the λ values were closer to 1.0 in long-lived species, while the short-lived species exhibited a wide range of λ values. This result confirms that all species are slowly declining, species with longer life-span at a slower rate (higher growth rate). Perhaps this is because individuals of these species are slowly dying in the same order as the life-span (about 9%, 11%, 11% and 13% respectively for *A. schirensis*, *A. canaliculatus*, *H. diplandra* and *L. simplex*; Table A1). There is thus a clear gradient in the life-span of the four species. Such a gradient together with other demographic differences could potentially be explained by non-documented differences in traits such as: the water and nutrient use efficiencies, the photosynthesis efficiency, phenology, and classical root and leaf traits in relation (Violle et al., 2007).

4.3. Interannual variability in demography of grass species

According to the log-linear analysis, the population transition matrix of each grass species varied significantly between years. This confirms that the demography of the four grass species varies from year-to-year as it is generally the case in perennial grasses (Horvitz and Schemske, 1995; Jongejans and De Kroon, 2005). This result is also confirmed by the LTRE analysis that shows that stasis, growth and retrogression contributed more to this temporal variation than fecundity. These interannual variations in the grass demography could be explained by the temporal variations of the climatic conditions that change from year to year in Lamto savanna (Le Roux, 2006). For example, the rainfalls during these three study years were 1478 mm, 951 mm and 1077 mm respectively in 2015, 2016 and 2017 (data from the Lamto geophysical station) and the populations of all species except *L. simplex* increased ($\lambda > 1.0$), but not significantly during the transition 1 (2015–2016) by at least 4%. Thus, the higher growth rates of these species in 2015 could be due to the higher amount of rain during this year 2015. Such a quantity of rain would have favoured the stasis and the growth of the individuals while disfavouring the retrogression. The fact that the population of *A. schirensis* and *H. diplandra* declined by 4% and 9% respectively during the two following transitions (≈1000 mm of rain) reinforces this hypothesis. *A. canaliculatus* and *L. simplex* seem to appreciate low rainfall since their highest growth rates were in low rainfall years. This is particularly clear in *L. simplex*, where the population increased by 7% when the rainfall dropped to 951 mm while it declined by 26% when the rainfall was the highest in 2015.

In these species, the climatic conditions could also have indirectly affected the temporal variations of the population through the intensity of the annual fire (Savadogo et al., 2007; Williams et al., 1998). Indeed, changes in rainfall can cause variations in the intensity of the yearly fire that has always been used for the management of the reserve (Frost et al., 1986; N'Dri et al., 2018). For example, low rainfall would cause low primary production and therefore a small amount of biomass i.e. fuel (Gignoux et al., 2006), which would lead to lower fire intensity and would have a lower impact on the grass demography (Trollope et al., 2002). However, this relationship between rainfall, fire intensity and temporal variations in grass demographic parameters remains to be proven and deepened by new statistical models using fire intensity and meteorological data. This would ideally require accumulating data for more yearly transitions.

4.4. Are the age parameters homogeneous between the grass circumference classes?

In all species, the mean age of individuals and the mean ages of residence in the classes were rather homogeneous from the class 2 to the class 5. This could be due to the fragmentation and the retrogression we observed in all species, particularly in larger individuals. Due to these two demographic parameters, the small size individuals are not always young but have the age of the large individuals from which they are the fragments (Gignoux et al., 2006). The weak differences observed between the size-classes (from class 2 to class 5) in each species are likely due to retrogression and fragmentation. Indeed, individuals can grow and retrogress several times before dying. This contributes to homogenise age-based parameters between circumference classes. This is confirmed by the fact that, for all classes, the standard deviations of ages are of the same order of magnitude as the mean age: the relation between size and age is blurred by retrogression and fragmentation. This also leads to the fact that the standard deviations of life-spans (the conditional remaining life-span (Ω_i) and total conditional life-span (Λ_i)) are higher than the life-spans, which denotes the high variability in the fate of the individuals within the same size-class: some individuals have just arrived from the first time in a given size-class, while others have already reached this class several times. On the other hand, the lower values of the age parameters obtained in the class 1 are due to the fact that the concerned individuals grow fairly quickly into the larger size-classes or die due to the small size and high growth rates of these individuals.

5. Conclusion

Despite the fact that the four studied species have the same general life-form and share the same environmental conditions, many demographic differences exist between their λs, age-based parameters and elasticity of the λs, which could help to understand differences in their dynamics. Moreover, the four grass populations have not fully attained their demographic equilibrium (differences between the observed and

predicted size-class distributions) after more than 50 years of the institution of the reserve, but three out of the four studied species are close to it (asymptotic grow rate not significantly different from 1.0). The demography of these grass species changes from year to year probably due to annual variations in climate and consecutive changes in fire intensity, which could contribute to explain why the grass populations are not at their demographic equilibrium. The most influential demographic parameter for the four grass species was stasis. Retrogression and fragmentation contribute to a certain homogeneity of the age parameters, from classes 2 to 5. However, we should monitor the grass populations for a few more years to better analyse the causes of the temporal variability in their demography. All the information collected could then be used to determine the mechanisms of coexistence (Barot and Gignoux, 2004) between savanna grass species. For example, coexistence should be favoured if interannual increases and decreases in λs are not synchronised between species. Monitoring the populations for more years would also allow better assessing the stability of the coexistence and the environmental factors responsible for interannual variations in the demography of the grass species.

Interestingly, savannas are based on the coexistence between trees and grasses and in humid savannas of West Africa, these grasses are perennial tussock grasses as in Lamto savanna. Though trees and grasses have different strategies to cope with fires we have shown that grasses might live as long as trees and, for this, reason they probably share some common demographic features. However, a difference between trees and grasses is that in trees retrogression tends to be limited to young individuals that resprout each year when fire has burnt down their aboveground parts. Older and larger trees become resistant to fire and their aboveground biomass no longer burns each year. In the same vein, grasses incur fragmentation, which is not the case for trees. The impact of these differences could be better understood by comparing thoroughly tree and grass matrix models.

Declaration of competing interest

The authors declare that they have no known competing financial interests or personal relationships that could have appeared to influence the work reported in this paper.

Acknowledgements

This research was supported by the Direction of Research and Training in the South of the Institute of Research for Development (IRD-DPF) [PhD grant to K.F.K.]. Thanks to Professor Yéo Kolo, the Director of the Lamto ecology station, for hosting us. Thanks to the Lamto geophysical station who gave us free, the meteorological data used in this work. Thanks to Tionhonkélé Drissa Soro, Koffi Prosper Kpangba, Koffi Sylvain Yoboué and Aka Jean-Noël Kpré for help during data collection. Thanks to the projects in which this study was conducted: ‘‘Integrated and Sustainable Management of Savanna Ecosystems’’ (GIDES) funded by the IRD within the “Young Associated Team” (JEAI) program and “Impact de la diversité des Graminées et ligneux de savane sur la diversité microbienne et le fonctionnement des sols” funded by the French national program EC2COMicrobiEn 2014.

Appendix A. Supplementary data

Supplementary data to this article can be found online at https://doi.org/10.1016/j.actao.2022.103816.

References

Abbadie, L., Gignoux, J., Lepage, M., Le Roux, X., 2006. Environmental constraints on living organisms. In: Abbadie, L., Gignoux, J., Le Roux, X., Lepage, M. (Eds.), Lamto, Ecological Studies. Springer, New York, pp. 45–61. https://doi.org/10.1007/0-387-33857-8_4.

Ariza, C., Tielbörger, K., 2011. An evolutionary approach to studying the relative importance of plant–plant interactions along environmental gradients. Funct. Ecol. 25, 932–942. https://doi.org/10.1111/j.1365-2435.2011.01848.x.

Barot, S., Gignoux, J., 2004. Mechanisms promoting plant coexistence: can all the proposed processes be reconciled? Oikos 106, 185–192. https://doi.org/10.1111/j.0030-1299.2004.13038.x.

Barot, S., Gignoux, J., Legendre, S., 2002. Stage-structured matrix models and age estimates. Oikos 96, 56–61.

Barot, S., Gignoux, J., Legendre, S., Vuattoux, R., 2000. Demography of a savanna palm tree in Ivory Coast (Lamto): population persistence, and life history. J. Trop. Ecol. 16, 637–655.

Boudsocq, S., Lata, J.C., Mathieu, J., Abbadie, L., Barot, S., 2009. Modelling approach to analyse the effects of nitrification inhibition on primary production. Funct. Ecol. 23, 220–230. https://doi.org/10.1111/j.1365-2435.2008.01476.x.

Brink, M., Achigan-Dako, E.G., 2012. Plantes à fibres. PROTA.

Brys, R., Jacquemyn, H., De Blust, G., 2005. Fire increases aboveground biomass, seed production and recruitment success of *Molinia caerulea* in dry heathland. Acta Oecol. 28, 299–305. https://doi.org/10.1016/j.actao.2005.05.008.

Buckley, Y.M., Ramula, S., Blomberg, S.P., Burns, J.H., Crone, E.E., Ehrlén, J., Knight, T.M., Pichancourt, J.-B., Quested, H., Wardle, G.M., 2010. Causes and consequences of variation in plant population growth rate: a synthesis of matrix population models in a phylogenetic context: plant population dynamics in space and time. Ecol. Lett. 13, 1182–1197. https://doi.org/10.1111/j.1461-0248.2010.01506.x.

Burns, J.H., Blomberg, S.P., Crone, E.E., Ehrlén, J., Knight, T.M., Pichancourt, J.-B., Ramula, S., Wardle, G.M., Buckley, Y.M., 2010. Empirical tests of life-history evolution theory using phylogenetic analysis of plant demography. J. Ecol. 98, 334–344. https://doi.org/10.1111/j.1365-2745.2009.01634.x.

Butler, J.L., Briske, D.D., 1988. Population structure and tiller demography of the bunchgrass *Schizachyrium scoparium* in response to herbivory. Oikos 51, 306–312. https://doi.org/10.2307/3565311.

Caswell, H., 2001. Matrix Population Models: Construction, Analysis, and Interpretation. Sinauer Associates Inc., Sunderland.

Caswell, H., 1996. Analysis of life table response experiments II. Alternative parameterizations for size- and stage-structured models. Ecol. Model. 88, 73–82. https://doi.org/10.1016/0304-3800(95)00070-4.

Caswell, H., 1989. Matrix Population Models. Sinauer Associates Inc., Sunderland.

Cochran, M.E., Ellner, S., 1992. Simple methods for calculating age-based life history parameters for stage-structured populations. Ecol. Monogr. 62, 345–364. https://doi.org/10.2307/2937115.

Crone, E.E., Menges, E.S., Ellis, M.M., Bell, T., Bierzychudek, P., Ehrlén, J., Kaye, T.N., Knight, T.M., Lesica, P., Morris, W.F., Oostermeijer, G., Quintana-Ascencio, P.F., Stanley, A., Ticktin, T., Valverde, T., Williams, J.L., 2011. How do plant ecologists use matrix population models? Ecol. Lett. 14, 1–8. https://doi.org/10.1111/j.1461-0248.2010.01540.x.

De Kroon, H., Groenendael, J.V., Ehrlen, J., 2000. Elasticities: a review of methods and model limitations. Ecology 81, 607–618.

Durán Zuazo, V.H., Rodríguez Pleguezuelo, C.R., 2008. Soil-erosion and runoff prevention by plant covers. A review. Agron. Sustain. Dev. 28, 65–86. https://doi.org/10.1051/agro:2007062.

Fingleton, B., 1984. Models of Category Counts. Cambridge University Press.

Frost, P., Medina, E., Ménaut, J.C., Solbrig, O., Swift, M., Walker, B., 1986. Responses of savannas to stress and disturbance: a proposal for a collaborative programme of research, IUBS, UNESCO MAB. In: Frost, Peter, Menaut, Jean-Claude, Walker, Brian, Medina, Ernesto, Solbrig, Otto T., Swift, Michael (Eds.), Biology International.

Garnier, L.K., Durand, J., Dajoz, I., 2002. Limited seed dispersal and microspatial population structure of an agamospermous grass of West African savannahs, Hyparrhenia diplandra (Poaceae). Am. J. Bot. 89, 1785–1791.

García, M.B., Picó, F.X., Ehrlén, J., 2008. Life span correlates with population dynamics in perennial herbaceous plants. Am. J. Bot. 95, 258–262. https://doi.org/10.3732/ajb.95.2.258.

Garnier, L.K.M., Dajoz, I., 2001. The influence of fire on the demography of a dominant grass species of West African savannas, *Hyparrhenia diplandra*. J. Ecol. 89, 200–208. https://doi.org/10.1046/j.1365-2745.2001.00532.x.

Gignoux, J., Barot, S., Menaut, J.-C., Vuattoux, R., 2006. Structure, long-term dynamics, and demography of the tree community. In: Lamto, Ecological Studies. Springer, pp. 335–364.

Harun, N., Chaudhry, A.S., Shaheen, S., Ullah, K., Khan, F., 2017. Ethnobotanical studies of fodder grass resources for ruminant animals, based on the traditional knowledge of indigenous communities in Central Punjab Pakistan. J. Ethnobiol. Ethnomed. 13, 56. https://doi.org/10.1186/s13002-017-0184-5.

Harvell, C.D., Caswell, H., Simpson, P., 1990. Density effects in a colonial monoculture: experimental studies with a marine bryozoan (*Membranipora membranacea* L.). Oecologia 82, 227–237. https://doi.org/10.1007/BF00323539.

Hoffmann, W.A., 1999. Fire and population dynamics of woody plants in a neotropical savanna: matrix model projections. Ecology 80, 1354–1369.

Horvitz, C.C., Schemske, D.W., 1995. Spatiotemporal variation in demographic transitions of a tropical understory herb: projection matrix analysis. Ecol. Monogr. 65, 155–192. https://doi.org/10.2307/2937136.

Huenneke, L.F., Marks, P.L., 1987. Stem dynamics of the shrub *Alnus incana* ssp. *rugosa*: transition matrix models. Ecology 68, 1234–1242. https://doi.org/10.2307/1939207.

Jongejans, E., De Kroon, H., 2005. Space versus time variation in the population dynamics of three co-occurring perennial herbs. J. Ecol. 93, 681–692. https://doi.org/10.1111/j.1365-2745.2005.01003.x.

Koffi, K.F., N'Dri, A.B., Lata, J.-C., Konaté, S., Srikanthasamy, T., Konan, M., Barot, S., 2019a. Effect of fire regime on the grass community of the humid savanna of Lamto. Ivory Coast. J. Trop. Ecol. 35, 1–7. https://doi.org/10.1017/S0266467418000391.

Koffi, K.F., N'Dri, A.B., Lata, J.-C., Konaté, S., Srikanthasamy, T., Konaré, S., Konan, M., Barot, S., 2019b. Effect of fire regimes on the demographic parameters of the perennial tussock grasses of a humid savanna. J. Veg. Sci. 30, 950–962. https://doi.org/10.1111/jvs.12788.

Kort, J., Collins, M., Ditsch, D., 1998. A review of soil erosion potential associated with biomass crops. Biomass Bioenergy 14, 351–359. https://doi.org/10.1016/S0961-9534(97)10071-X.

Lamotte, M., Tireford, J.-L., 1988. Le climat de la savane de Lamto (Côte d'Ivoire) et sa place dans les climats de l'Ouest africain. Université d'Abidjan, Station d'Ecologie Tropicale de Lamto, N'douci, Côte d'Ivoire.

Lauenroth, W.K., Adler, P.B., 2008. Demography of perennial grassland plants: survival, life expectancy and life span: demography of grassland plants. J. Ecol. 96, 1023–1032. https://doi.org/10.1111/j.1365-2745.2008.01415.x.

Le Roux, X., 2006. Climate. In: Lamto, Ecological Studies. Springer, New York, pp. 25–44.

Lefkovitch, L.P., 1965. The study of population growth in organisms grouped by stages. Biometrics 21, 1–18. https://doi.org/10.2307/2528348.

Menaut, J.-C., Abbadie, L., 2006. Vegetation. In: Abbadie, L., Gignoux, J., Le Roux, X., Lepage, M. (Eds.), Lamto, Ecological Studies. Springer, New York, pp. 63–74. https://doi.org/10.1007/0-387-33857-8_5.

Moloney, K.A., 1988. Fine-scale spatial and temporal variation in the demography of a perennial bunchgrass. Ecology 69, 1588–1598. https://doi.org/10.2307/1941656.

Murphy, B.P., Bowman, D.M.J.S., 2012. What controls the distribution of tropical forest and savanna?: tropical forest and savanna distribution. Ecol. Lett. 15, 748–758. https://doi.org/10.1111/j.1461-0248.2012.01771.x.

N'Dri, A.B., Soro, T.D., Gignoux, J., Dosso, K., Koné, M., N'Dri, J.K., Koné, N.A., Barot, S., 2018. Season affects fire behavior in annually burned humid savanna of West Africa. Fire Ecol 14, 1–11. https://doi.org/10.1186/s42408-018-0005-9.

O'Connor, T.G., 1993. The influence of rainfall and grazing on the demography of some African savanna grasses: a matrix modelling approach. J. Appl. Ecol. 30, 119–132. https://doi.org/10.2307/2404276.

Salguero-Gómez, R., De Kroon, H., 2010. Matrix projection models meet variation in the real world. J. Ecol. 98, 250–254. https://doi.org/10.1111/j.1365-2745.2009.01635.x.

Sankaran, M., Hanan, N.P., Scholes, R.J., Ratnam, J., Augustine, D.J., Cade, B.S., Gignoux, J., Higgins, S.I., Le Roux, X., Ludwig, F., Ardo, J., Banyikwa, F., Bronn, A., Bucini, G., Caylor, K.K., Coughenour, M.B., Diouf, A., Ekaya, W., Feral, C.J., February, E.C., Frost, P.G.H., Hiernaux, P., Hrabar, H., Metzger, K.L., Prins, H.H.T., Ringrose, S., Sea, W., Tews, J., Worden, J., Zambatis, N., 2005. Determinants of woody cover in African savannas. Nature 438, 846–849. https://doi.org/10.1038/nature04070.

Savadogo, P., Zida, D., Sawadogo, L., Tiveau, D., Tigabu, M., Oden, P.C., 2007. Fuel and fire characteristics in savanna-woodland of West Africa in relation to grazing and dominant grass type. Int. J. Wildland Fire 16, 531–539. http://www.publish.csiro.au/paper/WF07011.htm.

Schleuning, M., Matthies, D., 2009. Habitat change and plant demography: assessing the extinction risk of a formerly common grassland perennial. Conserv. Biol. 23, 174–183. https://doi.org/10.1111/j.1523-1739.2008.01054.x.

Shea, R.W., Shea, B.W., Kauffman, J.B., Ward, D.E., Haskins, C.I., Scholes, M.C., 1996. Fuel biomass and combustion factors associated with fires in savanna ecosystems of South Africa and Zambia. J. Geophys. Res. Atmos. 101, 23551–23568. https://doi.org/10.1029/95JD02047.

Silva, J.F., Raventos, J., Caswell, H., Trevisan, M.C., 1991. Population responses to fire in a tropical savanna grass, *Andropogon semiberbis*: a matrix model approach. J. Ecol. 79, 345–355. https://doi.org/10.2307/2260717.

Silvertown, J., Franco, M., McConway, K., 1992. A demographic interpretation of Grime's triangle. Funct. Ecol. 6, 130. https://doi.org/10.2307/2389746.

Silvertown, J., Franco, M., Pisanty, I., Mendoza, A., 1993. Comparative plant demography-relative importance of life-cycle components to the finite rate of increase in woody and herbaceous perennials. J. Ecol. 81, 465–476. https://doi.org/10.2307/2261525.

Soro, T.D., Koné, M., N'Dri, A.B., N'Datchoh, E.T., 2021. Identified main fire hotspots and seasons in Côte d'Ivoire (West Africa) using MODIS fire data. South Afr. J. Sci. 117, 1–13. https://doi.org/10.17159/sajs.2021/7659.

Srikanthasamy, T., Leloup, J., N'Dri, A.B., Barot, S., Gervaix, J., Koné, A.W., Koffi, K.F., Le Roux, X., Raynaud, X., Lata, J.-C., 2018. Contrasting effects of grasses and trees on microbial N-cycling in an African humid savanna. Soil Biol. Biochem. 117, 153–163.

Stokes, K.E., Bullock, J.M., Watkinson, A.R., 2004. Population dynamics across a parapatric range boundary: *Ulex gallii* and *Ulex minor*. J. Ecol. 92, 142–155. https://doi.org/10.1111/j.1365-2745.2004.00844.x.

Strohbach, B.J., Walters, H.J.A., Wally, 2015. An overview of grass species used for thatching in the Zambezi, Kavango East and Kavango west regions, Namibia. Dinteria 35, 13–42.

Tessema, Z.K., de Boer, W.F., Prins, H.H.T., 2016. Changes in grass plant populations and temporal soil seed bank dynamics in a semi-arid African savanna: Implications for restoration. J. Environ. Manag. 182, 166–175. https://doi.org/10.1016/j.jenvman.2016.07.057.

Tiemoko, D.T., Yoroba, F., Diawara, A., Kouadio, K., Kouassi, B.K., Yapo, A.L.M., 2020. Understanding the local carbon fluxes variations and their relationship to climate conditions in a sub-humid savannah-ecosystem during 2008-2015: case of Lamto in Cote d'Ivoire. Atmos. Clim. Sci. 10, 186–205. https://doi.org/10.4236/acs.2020.102010.

Trollope, W.S.W., Trollope, L.A., Hartnett, D.C., 2002. Fire behaviour a key factor in the fire ecology of African grasslands and savannas. In: Forest Fire Research and Wildland Fire Safety. Millpress Science Publishers, Rotterdam, Netherlands, pp. 1–15.

Tuljapurkar, S., Horvitz, C.C., Pascarella, J.B., 2003. The many growth rates and elasticities of populations in random environments. Am. Nat. 162, 489–502. https://doi.org/10.1086/378648.

Violle, C., Navas, M.-L., Vile, D., Kazakou, E., Fortunel, C., Hummel, I., Garnier, E., 2007. Let the concept of trait be functional. Oikos 116, 882–892. https://doi.org/10.1111/j.0030-1299.2007.15559.x.

Whelan, R.J., 1995. The Ecology of Fire. Cambridge University Press, Cambridge ; New York, USA.

Williams, R.J., Gill, A.M., Moore, P.H.R., 1998. Seasonal changes in fire behaviour in a tropical savanna in Northern Australia. Int. J. Wildland Fire 8, 227–239. https://doi.org/10.1071/wf9980227.